Electrical Power and Energy Systems 166 (2025) 110554

Contents lists available at ScienceDirect

International Journal of Electrical Power and Energy Systems

journal homepage: www.elsevier.com/locate/ijepes

Smart rail power systems: From the local to the centralised control operating paradigm

Antonio Di Pasquale *, Mario Pagano

Department of Information Technology and Electrical Engineering, University of Naples Federico II, Via Claudio 21, Naples, 80125, Italy

ARTICLE INFO

Keywords:
Smart railway system
Local control
Centralised control
Optimal power flow

ABSTRACT

Despite extensive scientific literature on the smart grid concept for buildings, neighbourhoods, and cities, the concept of Smart Railway Systems (SRSs) remains only partially explored. As a result, this work lays the foundation for implementing the smart paradigm in traction power systems for urban applications (i.e., metro and light rail transit systems). It introduces a modern control paradigm where the supervisor exchanges data with the sub-systems (i.e., trains, energy storage systems, and substations) and defines local controllers' set points according to optimisation strategies. Depending on the system's configuration, two control strategies, framed as optimal power flow problems, are proposed. The effectiveness of these strategies is assessed through a comprehensive numerical analysis, where real data from Naples Line 1 metro serve as a case study.

1. Introduction

Social and economic analysis estimate that the percentage of people living in urbanised areas is expected to grow from 55% to 70% in the next years [1]. As a result, several studies indicate that the increasing urban population will lead to rising demand for urban transport (i.e., ranging from 60% to 90% [2]). In this scenario, insufficient local public transportation options could inevitably lead to a significant reliance on road transport, which currently contributes to most of the environmental pollution in urban areas [3]. In this context, the railway system, as one of the most efficient modes of urban transportation, plays a pivotal role in promoting urban sustainability. Particularly, city planners and railway system operators will soon need to face complex decisions as they strive to enhance the capacity of the current Urban Rail Systems (URSs). Achieving this objective necessitates a focused effort on enhancing the efficiency of entire railway infrastructures.

Since the 2000s, the scientific literature has extensively explored this subject, proposing various measures, including the installation of Energy Storage Systems (ESSs) on-board or wayside, as well as the implementation of new controllable Traction Substations (TSSs). For instance, [4,5] investigated the potential energy savings achievable through On-board Energy Storage Systems (OESSs) in the case of the Brussels tram and metro lines, respectively. Similar studies were conducted on the Madrid metro line [6], Blackpool tramway [7], Mannheim tramway [8] and Paris tram line [9]. Notably, these analyses disclosed energy-saving rates ranging from 16% to 35.8%. Similar analyses were conducted in the case of Wayside Energy Storage Systems (WESSs) solutions, which, compared with on-board systems, offer the advantage of fewer limitations regarding weight and spatial requirements. Moreover, they can absorb the braking energy simultaneously injected by several vehicles and enhance the network voltage stability [10]. In this respect, [11] conducted a numerical assessment of the energy savings achievable through a supercapacitor WESS located at the TSSs of the Tehran metro line 3. The daily estimated energy savings amounted to approximately 25%. Similarly, it was estimated that the adoption of supercapacitor wayside solutions in Brussels metro lines could provide energy savings ranging from 26.3% to 35.8% depending on different traffic scenarios [5]. [12] estimated that the installation of WESSs would significantly improve the efficiency of the Seoul Metro Line 7, resulting in an operation cost reduction of 28%.

Another valuable measure is represented by using reversible traction substations, which allow power exchanges between the traction network (typically in DC for urban applications) and the AC distribution grid. For instance, [13] detailed the relevant achievement obtained within the *RailEnergy* project, where simulation results showed that the installation of reversible substations could be able to improve the receptivity of the Dutch regional line Utrecht–Zwolle up to 99%, resulting in energy savings of approximately 7%. Recently, due to the technological development of power semiconductor IGBT and converter control, IGBT-based inverters have become a valuable cost-effective solution. Compared with ESSs, they offer several advantages in terms of space, cost, reliability and lifetime [14]. Notably, regenerative inverters have found application in over 20 metro lines in China. For

* Corresponding author.
E-mail address: antonio.dipasquale@unina.it (A. Di Pasquale).

https://doi.org/10.1016/j.ijepes.2025.110554
Received 19 April 2024; Received in revised form 14 August 2024; Accepted 18 February 2025
Available online 11 March 2025
0142-0615/

Nomenclature

DSO	Distribution System Operator
ESS	Energy Storage System
OESS	Onboard Energy Storage System
OTPF	Optimal Traction Power Flow
PCC	Point of Common Coupling
RBE	Regenerative Braking Energy
REM-S	Railway Energy Management System
RPFMS	Railway Power Flow Management System
RSO	Railway System Operator
SG	Smart Grid
SRS	Smart Rail System
STD	Smart Train Driving
TO	Traction Operator
TPS	Traction Power System
TSS	Traction Substation
URS	Urban Rail System
WESS	Wayside Energy Storage System

instance, in the Beijing Metro Line 10, the installation of two sets of 2 MW reversible converters yielded an average daily energy savings of 11.15% [15].

Nevertheless, while the construction of new infrastructure and the installation of additional devices offer relevant options, they come with significant time and cost implications. Additionally, the traction system faces challenges related to its adaptability, especially in accommodating fluctuations in transportation demand. In response to these challenges, some works suggest extending the Smart Grids (SGs) paradigm to rail transit systems. Adopting such a measure could significantly improve the efficiency and flexibility of existing systems. Furthermore, this approach does not dismiss the energy-efficient measures mentioned earlier; instead, combining this new paradigm with those solutions may further enhance the efficiency of the entire railway infrastructure. A literature review on the concept of Smart Rail System (SRS) and its applicability is provided in Section 2.

The present work fits into the context of SRSs. Its primary contributions can be summarised as follows:

- Demonstrating the key differences between conventional local control and centralised control in the realisation of SRSs.;
- Formulating a power flow model and designing centralised control strategies for optimal energy management of a URS, specifically examining two alternative URS configurations.
- Showcasing the proposed methods in a real case study, assessing the effectiveness of two alternative optimal control strategies framed as OTPF problems.

The remainder of the paper is organised as follows: Section 2 introduces the concept of SRS, emphasising the potential benefits derived from adopting the SG paradigm within the railway context. Additionally, Section 3 describes the control paradigm conventionally adopted in URSs, whereas Section 4 introduces the control paradigm based on the centralised control that forms the basis of the proposed SRS. Section 5 presents the mathematical model for the analysis of the railway system in terms of power flow approach. Additionally, it provides the theoretical fundamentals for the implementation of the Optimal Traction Power Flow (OTPF). Hence, Section 6 proposes the comparison of two alternative optimal control strategies framed as OTPF problems. The two strategies alternatively examine the cases of diode-based TSSs equipped with WESS and inverter-based TSSs. The effectiveness of the proposals is assessed through a numerical analysis carried out using real data of Metro Line 1 of Naples. The numerical results are highlighted and discussed in Section 7. Finally, Section 8 draws the main conclusions.

2. Related literature

URSs and, more in general, railway systems represent extensive distributed grid-connected complex systems, encompassing numerous distributed varying active loads (e.g., trains), substations either unidirectional or reversible and storage devices located both wayside and on-board. Consequently, the SG paradigm emerges as a particularly well-suited solution for the effective energy flow management of such a system. This concept has already demonstrated success in applications ranging from homes and buildings to city quarters and smart cities, which are examples of distributed systems aiming to achieve optimal energy scheduling [16–18].

The smart energy management of railway systems is a major challenge due to the inherent complexity of the technological system, the variety and time dependence conditions of operating scenarios and the strong requirements in terms of reliability, security and safety [19]. Despite the vast literature concerning SGs, the concept of a SRS has not been thoroughly investigated. Developing an SRS for managing energy flows among system's units could significantly enhance energy efficiency in the railway system, leading to improved service quality for users. Moreover, integrating the SG paradigm into railway systems can enhance resilience and flexibility. These aspects are especially crucial for accommodating fluctuations in transport demand, which align with economic trends within metropolitan cities, regions, and countries. For instance, increasing transport demand may push the system to its capacity limits, resulting in the need of managing transient overloads on certain line segments and/or counteracting significant voltage drops at specific locations. This can severely affect railway services during rush hours at specific sites. Typically, actual solutions involve costly upgrades to the Traction Power System (TPS) such as adding parallel conductors to the catenary or installing new substations and storage devices. While these measures are technically effective, they are costly and lack adaptability. Additionally, any future reduction in transport demand could make these measures not only expensive but also potentially inefficient.

In this regard, the SRS concept constitutes a more effective and flexible approach. It focuses on adjusting operations to prevent the system from reaching the prescribed limits in terms of overcapacity and ensure a high-quality service. The coordination among the control actions provided by trains, storage devices and substations can lead to significant energy savings, particularly through the efficient recovery of regenerative braking, which stands out as a primary solution for reducing the energy consumption of railway systems. In simple terms, the paradigm of centrally controlling power flow exchanges among the system's units can be seen as a natural extension of the supervision techniques already used for fleet motion safety, now applied to energy management requirements. (e.g., [20]).

It is important to note that the transition towards an SRS is a complex undertaking involving multiple stakeholders, namely the Railway System Operator (RSO) responsible for managing railway infrastructure, the Traction Operators (TO) specialising in freight and passenger transportation, and eventually, the DSO responsible for supplying the railway infrastructure, can be beneficiaries in terms of reducing costs, power requirements, power quality (e.g., [21]). Indeed, over the past decades, European countries have undergone significant rail sector reorganisation in response to various European Railway Packages aimed at liberalising the railway market, with the primary goal of fostering competition in the provision of railway services, thereby improving both efficiency and quality of service [22,23].

2.1. Smart operations

The development of an SRS passes through the implementation of smart management operations involving train fleets, TPS and upstream AC distribution grid. These operations can be applied at two distinct levels: traffic flow and traction power flow operations. In other words, the SG paradigm complies with the way trains move and are supplied. Hence, the smart management operations can be categorised as follows:

- *Smart train operation*: trains already serve as flexible tools for RSOs, which offline perform the optimisation of the speed profile depending on the features and the needs of the traction system. This process results in designing a set of driving strategies to be applied in the different journeys. However, to develop SRS, the next step is making this procedure online through a Smart Train Driving (STD) control, which can dynamically adapt the train speed according to the passenger demand and contingent factors such as network congestion, overload limits and network receptivity. More precisely, the STD employs an optimisation framework whose objective can be the minimisation of energy consumption, reduction of electricity cost or simply adapting the train speed profile to the capacity of the local traction network.
- *Smart traction power flow operation*: the advances in power electronics are encouraging the spread of storage devices as well as reversible substations, resulting in higher levels of controllability. In a smart context, trains, TSSs, onboard and wayside storage devices can be managed through an optimal power flow control, which, dynamically adjusts the output voltage of both TPSs and the wayside storage system to accommodate higher regenerative power or to counteract voltage sags. Similarly, the power that trains either consume or inject can be adjusted to mitigate voltage drops and maximise the usage of RBE.
- *Smart interaction with the distribution grid*: because of its significant size, the railway system does not have a negligible impact on the AC distribution grid operations. Hence, in a smart scenario, the RSO can also assist the DSO in online grid management. This support includes providing ancillary services and serving as a flexible load to address fluctuations in renewable energy resources or respond to contingency events, such as the loss of specific generation units or distribution lines [24].

The most relevant research in this context was carried out as part of the European MERLIN project, which aimed to investigate and demonstrate the feasibility of an integrated management system for achieving more sustainable and efficient energy usage in European electric mainline railway systems [25]. However, it is important to note that this project outlines the framework for realising an SRS but does not focus into the technological and operational details of smart power flow management.

2.2. Paper contribution

To the best of the authors' knowledge, the scientific literature lacks comprehensive investigations into the smart traction power flow operations mentioned above. This topic has only been partially investigated by researchers, who have either focused on small portions of the system or analysed the entire system without leveraging comprehensive mathematical models. For instance, [26] proposed an energy management strategy for a smart TSS considering regenerative braking and the stochastic behaviour of ESS and PV generation. However, this work looked only at the interaction between the TSS and the upstream distribution grid, without considering the simultaneous power exchanges involving trains, TSS, and ESSs. Similarly, [27] proposed an energy management system still limited to the control of a subway TSS, which was able to control its energy flow and ventilation airflow. [28] proposed a centralised power flow control strategy, but it was confined to managing the use of regenerative braking energy in a single section of an AC railway system between two TSSs. In [29], the authors examined a similar case involving three consecutive TSSs and also demonstrated that the time delays in communication systems meet the requirements for real-time control. Furthermore [30] introduced a coordinated control strategy for a multi-source traction system. This proposal manages the railway system through the conventional local control paradigm, whereas the optimisation lies in reducing peak power demand to the TSS by dynamically adjusting thresholds referring to the static operating characteristics of ESSs.

Moreover, as detailed in [19,31], the above-mentioned MERLIN project led to the development of the Railway Energy Management System (REM-S) integrating OESSs, WESSs, and coordination services to optimise energy usage within railway systems. The proposed architecture employs a hybrid centralised-decentralised approach, making use of SG concepts and the SGAM tools and framework. Notably, the viability of this approach was validated through a real-field test conducted on a suburban DC railway line in Malaga [32]. However, these works focus on a high-level energy-management framework which does not go into detail about the traction power flow operations. In this regard, a significant step forward has been made in [33], which introduced a centralised control strategy, formulated as an optimal power flow, for the energy management of URSs. Specifically, this approach considers as controllable variables the TSSs' power and the SoC of WESSs and provides some numerical comparison between the local control paradigm and the proposed centralised one. Inspired by [33], the present work aims to deepen the proposed approach by exploring the main differences between local and centralised control, using a more detailed modelling framework and introducing new controllable variables and objective functions. The main novelties of the present work compared with [33] can be summarised as follows:

- A detailed discussion on the local control paradigm and different types of local controllers (e.g. grid-following, grid-forming) applied to the different units (e.g., TSS, WESS and train).
- A detailed steady-state modelling framework. Specifically, a twofold model has been presented for each component of the URS, one under local control and the other under centralised control.
- Additional controllable variables have been introduced. The present work includes train regenerative power as a controllable variable along with different objective functions.
- The effectiveness of the proposed approach has been validated through numerical simulation performed on the real-case study of the entire Metro Line 1 of Naples.

3. Conventional urban rail systems management

Fig. 1 illustrates the typical configuration of an URS. As discussed in Section 2, in a non-vertically integrated market, two primary operators are involved: the RSO and TO. The former is responsible for managing both the power infrastructure and traffic flow of the fleet of trains, whereas the TO owns the rolling stock and pays the RSO for infrastructure utilisation and energy consumption.

From the RSO's perspective, the train fleet is considered a time-varying electric load to be supplied, whereas, from the TO's perspective, the RSO provides infrastructure and energy. Actually, these two operators do not actively collaborate for the optimal management of the traction system. Instead, they adopt a local control paradigm, with one side regulating the power delivered and the other side regulating the power drawn while maintaining the catenary voltage within the prescribed limits. This approach, although simple and effective, lacks the flexibility necessary to achieve a global optimisation of the traction system operations.

Particularly, it is possible to distinguish between two local control modes: *grid-following* and *grid-forming* [34]. These definitions are typically associated with converters operating in AC grids. Particularly, in

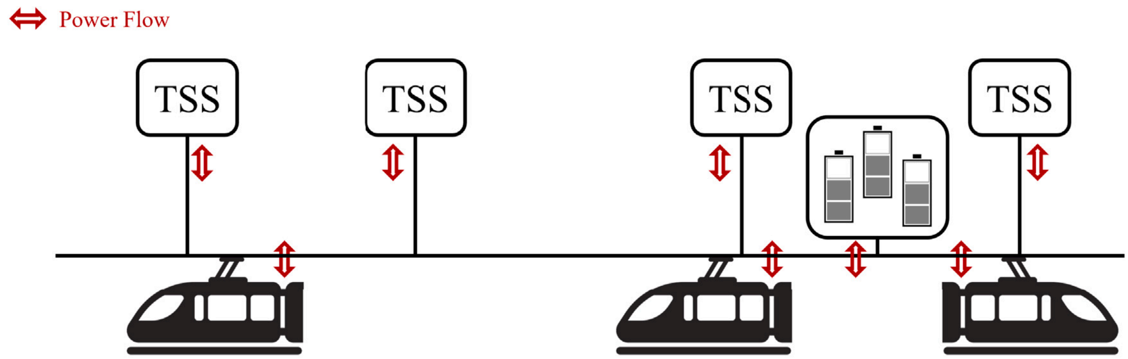

Fig. 1. Conventional URS configuration with TSS, trains and WESSs. The red arrows denote the power flow. Depending on the substation configuration it can be bidirectional or not.

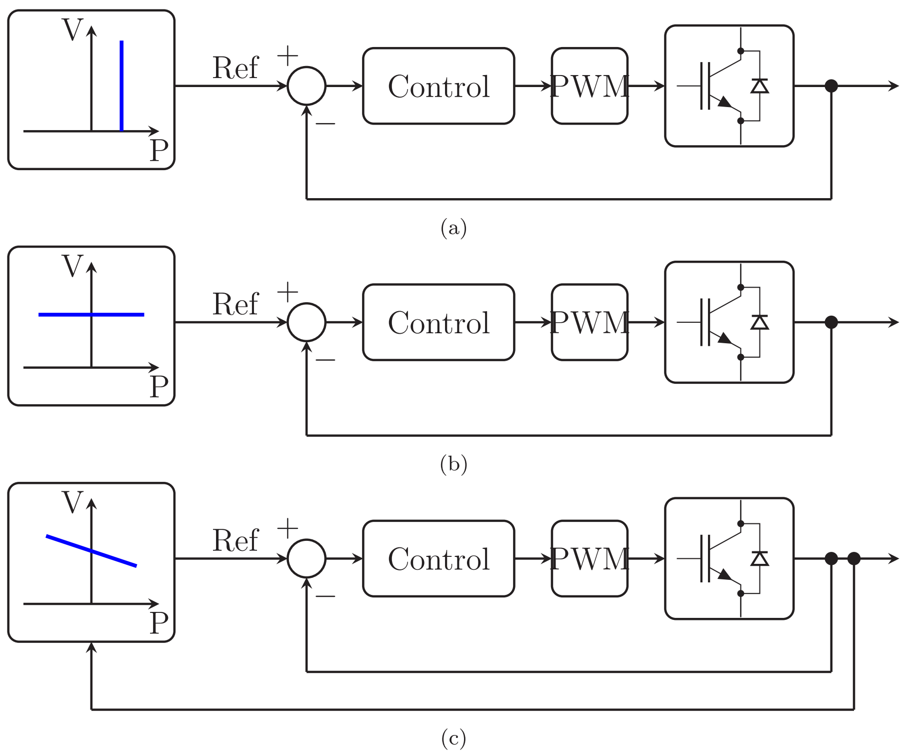

Fig. 2. Local control schemes: (a) grid-following mode, (b) grid-forming mode and (c) droop-controlled grid-forming mode.

grid-following mode, the current injected by the converter is controlled with a specific phase displacement from the grid voltage at the Point of Common Coupling (PCC). On the other hand, grid-forming units control the magnitude and angle of the voltage at the PCC [35]. It is worth noting that the grid-following operation is associated with the injection of the required amount of active and reactive power or with the control of the RMS voltage value. Conversely, the grid-forming operation is associated with frequency regulation and voltage supply establishment.

Remarkably, [36] extends the use of these terms to the case of DC traction systems. Grid-following mode refers to the capability of converters to act as ideal current sources, adjusting the current based on power demand and voltage. Alternatively, grid-forming mode denotes the capability of traction converters to operate as ideal voltage sources, which set, within certain limits, the value of voltage regardless of the power delivered. The control schemes for these two control modes are illustrated in Figs. 2(a) and 2(b). The key difference lies in the way the reference output is computed. It is important to note that trains and stationary storage systems often operate in grid-following mode. In the case of trains, the power reference primarily depends on the speed profile adopted. However, to prevent the catenary voltage from exceeding prescribed limits, trains adopt the squeeze control which, during the braking phase, reduces the amount of power injected into the network by wasting part of the RBE through the rheostatic braking system [37]. Conversely, in traction mode, the catenary voltage might drop below the lower limit. In these instances, the train's overcurrent protection reduces requested power, to safeguard the train's electrical components and limit catenary voltage drop [38,39]. Conversely, concerning WESSs, it is worth noting that, although in principle they could even operate in grid-forming mode, the grid-following operation is preferable since they operate in parallel with the traction substations and are primarily used to provide voltage support and load-levelling services. Thus, their reference power depends on the implemented voltage-current static characteristic, which, typically leads the storage discharging when the local catenary voltage falls below a certain value and charging when the catenary voltage rises.

On the other hand, controllable substations act as droop-controlled grid-forming converters, whose reference control scheme is reported in Fig. 2(c). More precisely, TSSs' reference voltage changes in response to the power delivered depending on the droop control parameter. This control law is very useful in parallel operating inverters as it enhances

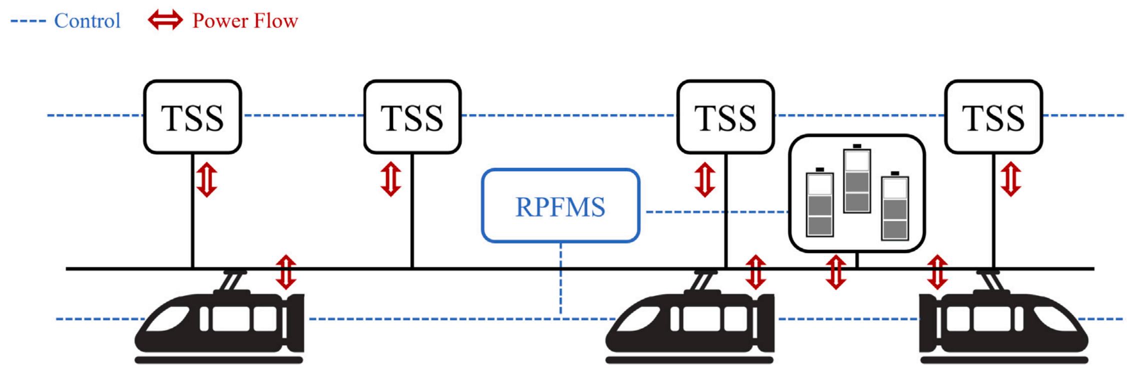

Fig. 3. The Smart Rail System scheme involves the RPFMS exchanging information with all sub-systems through a communication platform represented by the blue dotted line.

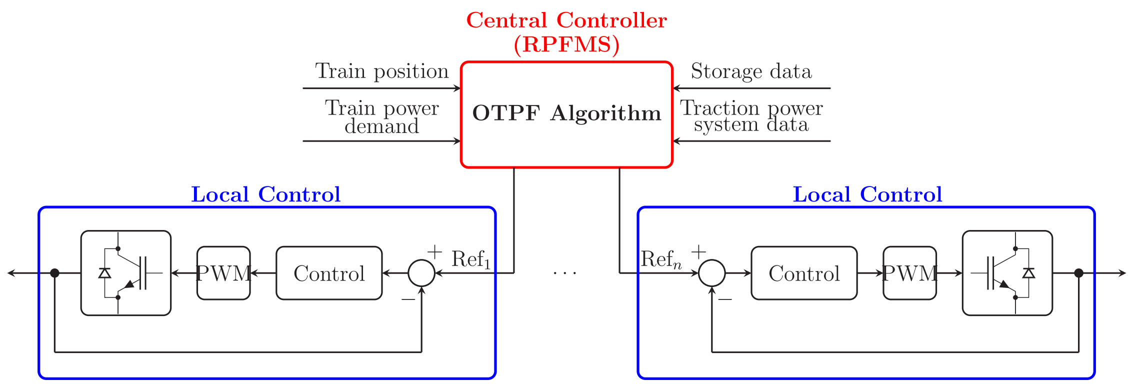

Fig. 4. Centralised control scheme: the central controller communicates with all agents and sets local controller set-points based on the optimisation problem.

proportional load sharing, contributes to the stability of the system and is relatively simple to implement. Furthermore, it is worth noting that this strategy offers the advantage of load-sharing based solely on droop control parameters and the distances between trains and substations. Remarkably, no traffic information is required.

4. Smart traction power flow operations

Among the various smart operations outlined in Section 2, this work focuses on smart traction power flow operations, which appear the most reasonable smart solution in the context of the earlier-discussed market liberalisation. Indeed, other smart operations, such as the STD approach, are not practical options in the current railway scenario. It is highly unrealistic to expect TO to provide the RSO with the capability to adjust train speeds based on factors such as network congestion, overload limits, and network receptivity. Conversely, smart traction power flow operations do not impact trains' dynamics but aim at optimising the exchange of power among trains as well as the charging/discharging power profile of storage devices installed either on-board or wayside.

Fig. 3 shows the reference architecture for the proposed SRS. This scheme differs from the conventional one depicted in Fig. 1, primarily due to the inclusion of a communication platform (indicated by the blue dotted line), enabling data exchange among various subsystems, including trains, TSSs and WESSs. Moreover, the control of the system is performed by a central controller called RPFMS (Railway Power Flow Management System), which is responsible for implementing online smart traction power flow operations using suitable control strategies. Subsequently, a set of control strategies for different system configurations is proposed.

Under local control, the regulation of powers, voltages and currents is carried out on local measurements. The lack of coordination among local controllers can lead to suboptimal management of power flows in the traction network. This, in turn, significantly impacts on the performance of the TPS, particularly on its ability to recover regenerative braking energy. In contrast, centralised control offers several advantages, primarily global optimisation. By enabling extensive data exchange with all connected devices, the central controller can take actions based on a comprehensive understanding of the operational states of each system. This allows for more efficient and effective management of the power system, overcoming the limitations of local control related to the limited receptivity of the network.

In alignment with the modern concept of SG, the present work proposes a centralised approach for the management of URSs. As illustrated in Fig. 4, the control scheme features a central controller, which establishes data exchange with various power systems, including trains, WESSs and substations. One key feature of this strategy is its online operation, requiring continuous data exchange between the controller and other systems. For instance, each time step (e.g., seconds) trains communicate to the central controller their position and the power that they are going to draw or inject. Simultaneously, the energy management systems of storage devices provide information on available energy and the current maximum charging and discharging power. Leveraging this data and based on the traction network model, the central controller solves an optimisation problem, whose solution provides optimised set points that are dispatched to all the local controllers. For instance, TSSs receive the reference value for their output voltage, storage devices the charging/discharging reference power, whereas braking trains the regenerative power that they have to inject into the network. Thus, the centralised nature of the control acts on the way the set points for local controllers are defined.

5. Rail power system modelling

This section establishes the fundamentals for power flow modelling of the DC TPS under both local and centralised control, emphasising

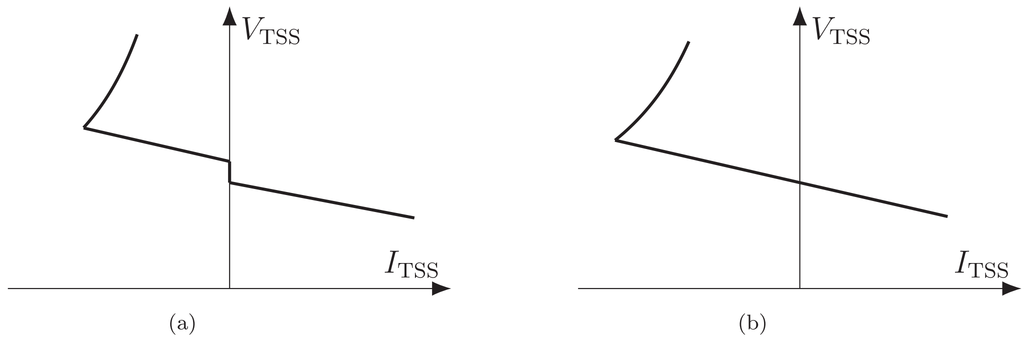

Fig. 5. Reversible TSS local control characteristics in the current–voltage plane: (a) hybrid configuration with four regions: rectifying, dead band, linear inverting, and inverting at constant power; (b) inverter-based solution lacking the dead-band region.

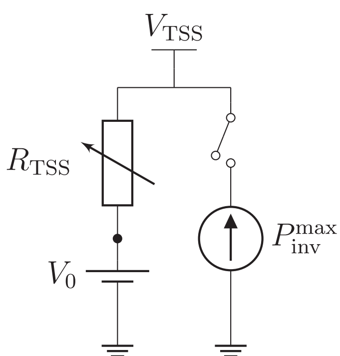

Fig. 6. TSS equivalent circuit.

key differences. Specifically, it outlines the steady-state models for the main subsystems of the URS, namely TSSs and WESSs, as well as the traction line and trains.

5.1. Traction substation

DC railway systems are typically connected to the AC distribution grid through TSSs consisting of a three-phase step-down transformer and an AC/DC converter. These transformers often feature on-load tap-changers, allowing for the adjustment of the output voltage. The AC/DC converters can be either diode bridge rectifiers or IGBT-based inverters, operating either independently or in parallel. More precisely, the TSS is called not-reversible when equipped solely with diode rectifiers, as power flows exclusively from the AC grid to the DC traction network. Conversely, the presence of inverters makes the TSS reversible, allowing bidirectional power flow. In particular, the reversible configuration can be realised either by connecting an inverter in parallel with the conventional diode-based TSS or by a single inverter. In the first setup, referred to as the hybrid configuration, the diode rectifier handles forward power flow, from the AC grid to the DC network, while the inverter manages reverse power flow, from the DC network to the AC grid. In the second setup, the inverter manages both forward power flow, and reverse power flow.

In this respect, Fig. 5 shows the reversible TSS operating characteristic under conventional local control. More precisely, it operates as a droop-controlled grid-forming converter. In the case of a hybrid configuration, the slope of the droop-control characteristic in the rectifying region is determined by the equivalent resistance of the diode bridge, which remains unmodifiable, whereas, in the inverting region, the droop coefficient is given by the desired value for the virtual resistance ($R_{\rm inv}$). On the other side, in purely inverter-based solutions the slope of the entire characteristic is given by the virtual impedance value.

Moreover, it is important to note that when the inverter approaches its maximum power, it operates along a curve at constant power. Hence, as depicted in Fig. 6, under the local control, as long as the transferred power is below the rated value, the equivalent model is an ideal voltage source with a voltage-driven resistance in series, whose value is given by:

$$R_{\rm TSS} = \begin{cases} R_{\rm rect} = \dfrac{V_0 - V_{\rm n}}{I_{\rm n}} & \text{if} \quad \Delta V_{\rm TSS} \geq 0 \\ R_{\rm off} \to \infty & \text{if} \quad -\Delta V_{\rm max} \leq \Delta V_{\rm TSS} < 0 \ \&\ P_{\rm TSS} > P_{\rm inv}^{\rm max} \\ R_{\rm inv} & \text{if} \quad \Delta V_{\rm TSS} < -\Delta V_{\rm max} \ \&\ P_{\rm TSS} > P_{\rm inv}^{\rm max} \end{cases} \tag{1}$$

where V_0 and $V_{\rm n}$ denote the TSS off-load and rated voltage, respectively. $\Delta V_{\rm TSS}$ represents the voltage drop across the TSS equivalent resistance, which is negative when the TSS output voltage exceeds the off-load voltage. In particular, in the hybrid configuration, a dead-band is defined to prevent leakage currents between the diode rectifier and the inverter. This dead-band separates the operations of the two converters, such that when $-\Delta V_{\rm max} \leq \Delta V_{\rm TSS} < 0$, (with $\Delta V_{\rm max}$ a fixed threshold) the diode rectifier is reversed-biased, and the inverter does not operate. Furthermore, it is important to note that when the transferred power reaches its maximum ($P_{\rm inv}^{\rm max}$), the model switches into a constant power source.

On the other side, under a centralised paradigm, the reversible TSS serves as a controllable device, whose set-points are provided by the central controller based on the implemented optimisation strategy. Specifically, in this framework, the TSS is modelled as a controllable voltage source, except for the rectifying region in the presence of a diode rectifier, which does not provide any controllable variable.

5.2. Wayside energy storage systems

When positioned alongside the track, WESSs offer voltage support to the DC TPS, effectively mitigating voltage drops caused by trains' high power demand and curtailing over-voltages during their braking phase. Alternatively, when installed at the TSS, they provide load-levelling functions. More precisely, under the conventional local control, they operate as a grid-following unit, whose typical voltage-power characteristic is shown in Fig. 7. The charging power is assumed negative and the discharging power is positive. Hence, the WESS is modelled as a voltage-dependent power load/generator whose power $P_{\rm sto}$ can be computed as follows:

$$P_{\rm sto} = \begin{cases} P_{\rm sto}^{\rm dis,av} & \text{if} \quad V_{\rm sto} < V_{\rm dis,con} \\ P_{\rm sto}^{\rm dis,av} \dfrac{V_{\rm sto} - V_{\rm db}^{\rm min}}{V_{\rm dis,con} - V_{\rm db}^{\rm min}} & \text{if} \quad V_{\rm dis,con} \leq V_{\rm sto} < V_{\rm db}^{\rm min} \\ 0 & \text{if} \quad V_{\rm dis,con} \leq V_{\rm db}^{\rm min} < V_{\rm db}^{\rm max} \\ P_{\rm sto}^{\rm ch,av} \dfrac{V_{\rm sto} - V_{\rm db}^{\rm max}}{V_{\rm ch,con} - V_{\rm db}^{\rm max}} & \text{if} \quad V_{\rm db}^{\rm max} \leq V_{\rm sto} < V_{\rm ch,con} \\ P_{\rm sto}^{\rm ch,av} & \text{if} \quad V_{\rm sto} \geq V_{\rm ch,con} \end{cases} \tag{2}$$

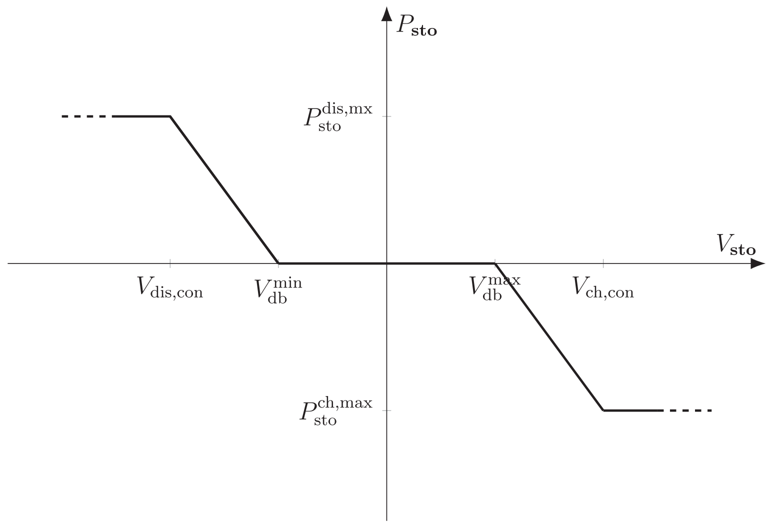

Fig. 7. Typical WESS static control characteristic. It features five operating regions: constant discharging power, constant charging power, linear discharging power, linear charging power, and the dead band.

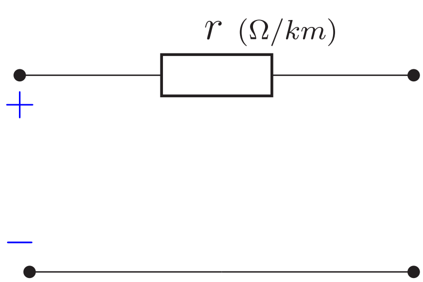

Fig. 8. Traction line simplified equivalent circuit, merging positive and return conductors.

where $P_{\text{sto}}^{\text{dis,av}}$ and $P_{\text{sto}}^{\text{ch,av}}$ represent the maximum value for the available discharging and charging power, respectively. These amounts of power vary according to the State of Charge (SoC) of the storage device. $V_{\text{db}}^{\text{min}}$ and $V_{\text{db}}^{\text{min}}$ define the dead-band region, within which the device does not operate, whereas $V_{\text{dis,con}}$ and $V_{\text{dis,con}}$ separate the linear discharging and charging zones from the constant discharging and charging zones, respectively.

On the other hand, under the centralised control paradigm, similar to the TSS, WESSs' set-points for the output voltage are provided by the central controller. Therefore, in this context, they are modelled as a controllable voltage source.

5.3. Traction line

The traction line in a DC URS generally consists of a messenger wire (e.g., one or two wires), a contact wire (e.g., one or two wires) and running rails. The messenger and contact wires are connected in parallel through droppers, forming an overhead catenary, which is connected to the positive busbar of the TSSs, supplying power to the trains. Alternatively, the overhead catenary can be replaced with a third rail, a rigid conductor positioned alongside or between the rails of the railway track. On the other side, running rails serve as the return path for traction current, connected to the TSS negative busbar. Despite insulation, leakage currents between the ground and the rail exist. The evaluation of these currents requires a complex model of the traction line, which involves an equivalent ladder network [40]. However, in power flow analysis, the primary goal is to determine train voltages and traction currents. Therefore, the extent of leakage current is considered negligible. As a result, a widely accepted approach involves modelling the traction line as a positive conductor, accounting for both the overhead catenary (or third rail) and running rails resistance, whereas an ideal return conductor establishes the reference for the voltages [37,41] (see Fig. 8). More precisely, the traction line is modelled with an equivalent per unit of length resistance (i.e., r (Ω/km)).

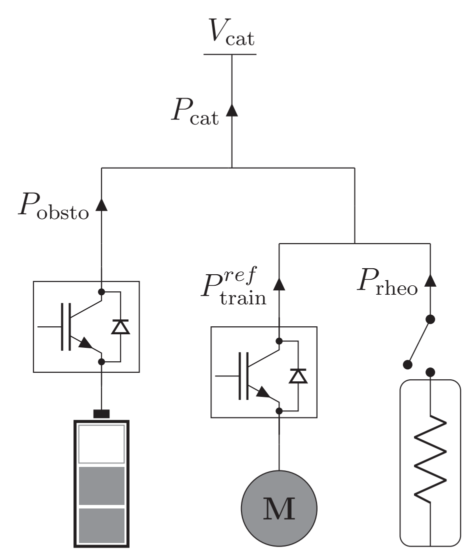

Fig. 9. Train model accounting for onboard storage system and rheostatic braking system.

5.4. Train

The train is the most complex device within the TPS. Typically, power flow analyses adopt a decoupled approach, according to which external software provides the train's mechanical power and position, serving as input to determine electrical variables. Notably, under this approach, factors like the train's position, speed profiles, and mechanical power are predetermined, regardless of the network's electrical state. However, the catenary voltage significantly affects the final values of absorbed or injected power by trains. For instance, during braking, RBE injection into the traction network could bring the catenary voltage exceeding its over-voltage limits. As discussed in Section 3, under local control, to prevent this event trains employ the squeeze-control, which depending on the catenary voltage dissipates the surplus of regenerative power. Conversely, in traction mode, the catenary voltage might drop below the lower limit. In these instances, the train's overcurrent protection reduces requested power, in order to safeguard the train's electrical components and limit catenary voltage drop [38,39]. Additionally, the final power injected or absorbed by the train depends on the presence of onboard storage devices, which perform power-smoothing operations. Typically, they supply as much power as possible during the train traction mode and conversely absorb as much regenerative power as possible during the train braking phase. More precisely, as illustrated in Fig. 9, the train's electrical power absorbed/injected at the catenary (P_{cat}) is given by the following expression:

$$P_{\mathrm{cat}} = P^{ref}_{\mathrm{train}} + P_{\mathrm{rheo}} + P_{\mathrm{obsto}} \tag{3}$$

where P^{ref}_{train} refers to the train reference power, derived from mechanical simulations and then converted into electrical power by considering the electro-mechanical efficiency. Additionally, P_{rheo} represents the power dissipated through the rheostatic braking system, and if present, P_{obsto} denotes the charging or discharging power of the OESS. It is important to note that according to the active sign convention, P_{rheo} is always lower or equal to zero. Additionally, the OESS charging power is assumed negative, whereas the discharging power is positive. Similarly, the power absorbed by the train during the traction phase is negative, whereas regenerative power is assumed positive.

Hence, under local control, the train is modelled as a voltage-dependent power load/generator, whose reference power is given by (3). In contrast, according to the centralised control paradigm, the train is modelled as a controllable power load/generator, as the OESS charging/discharging power as well as the train regenerative power can be controlled.

5.5. Traction power flow

Consider a generic DC railway traction network. Let $n \in \mathcal{N}$ denote the nodes of the network partitioned into three disjoints sets: $s \in \mathcal{S}$ the TSSs nodes, $b \in \mathcal{B}$ the WESSs nodes and $r \in \mathcal{R}$ the trains nodes. The power flow equations can be expressed in a compact way as follows:

$$\mathrm{diag}\,(\mathbf{V})\,\mathbf{G}\mathbf{V} = \mathbf{P} \tag{4}$$

where the operator diag gives a diagonal matrix, $\mathbf{V} \in \mathbb{R}^{|\mathcal{N}|}$ and $\mathbf{P} \in \mathbb{R}^{|\mathcal{N}|}$ are the nodal voltage and nodal injected power vectors, respectively, and $\mathbf{G} \in \mathbb{R}^{|\mathcal{N}|\times|\mathcal{N}|}$ is the compound conductance matrix. Notably, the latter captures the traction network topology, which varies along with the motion of the trains. More precisely, the introduced node partition leads to the following block-wise decomposition of the compound conductance matrix, as well as the nodal voltages and power vectors:

$$\mathrm{diag}\left(\begin{bmatrix}\mathbf{V}_{\mathcal{S}}\\ \mathbf{V}_{\mathcal{B}}\\ \mathbf{V}_{\mathcal{R}}\end{bmatrix}\right)\begin{bmatrix}\mathbf{G}_{\mathcal{S}\times\mathcal{S}} & \mathbf{G}_{\mathcal{S}\times\mathcal{B}} & \mathbf{G}_{\mathcal{S}\times\mathcal{R}}\\ \mathbf{G}_{\mathcal{B}\times\mathcal{S}} & \mathbf{G}_{\mathcal{B}\times\mathcal{B}} & \mathbf{G}_{\mathcal{B}\times\mathcal{R}}\\ \mathbf{G}_{\mathcal{R}\times\mathcal{S}} & \mathbf{G}_{\mathcal{R}\times\mathcal{B}} & \mathbf{G}_{\mathcal{R}\times\mathcal{R}}\end{bmatrix}\begin{bmatrix}\mathbf{V}_{\mathcal{S}}\\ \mathbf{V}_{\mathcal{B}}\\ \mathbf{V}_{\mathcal{R}}\end{bmatrix} = \begin{bmatrix}\mathbf{P}_{\mathcal{S}}\\ \mathbf{P}_{\mathcal{B}}\\ \mathbf{P}_{\mathcal{R}}\end{bmatrix} \tag{5}$$

where $\mathbf{V}_{\mathcal{S}} \in \mathbb{R}^{|\mathcal{S}|}$, $\mathbf{V}_{\mathcal{B}} \in \mathbb{R}^{|\mathcal{B}|}$, $\mathbf{V}_{\mathcal{R}} \in \mathbb{R}^{|\mathcal{R}|}$ are the TSSs, WESSs and trains nodal voltage vectors, respectively. On the other hand, $\mathbf{P}_{\mathcal{S}} \in \mathbb{R}^{|\mathcal{S}|}$, $\mathbf{P}_{\mathcal{B}} \in \mathbb{R}^{|\mathcal{B}|}$, $\mathbf{P}_{\mathcal{R}} \in \mathbb{R}^{|\mathcal{R}|}$ are the TSSs, WESSs and trains nodal power vectors, respectively. The blocks of matrix $\mathbf{G}$ are defined accordingly. Consequently, the traction power flow results in funding the roots of the non-linear function $\mathbf{F} : \mathbb{R}^{|\mathcal{N}|} \to \mathbb{R}^{|\mathcal{N}|}$ defined as follows:

$$\mathbf{F} = \begin{bmatrix}\mathbf{F}_{\mathcal{S}}\\ \mathbf{F}_{\mathcal{B}}\\ \mathbf{F}_{\mathcal{R}}\end{bmatrix} \tag{6}$$

where the functions $\mathbf{F}_{\mathcal{S}} \in \mathbb{R}^{|\mathcal{S}|\times 1}$, $\mathbf{F}_{\mathcal{B}} \in \mathbb{R}^{|\mathcal{B}|\times 1}$ and $\mathbf{F}_{\mathcal{R}} \in \mathbb{R}^{|\mathcal{R}|\times 1}$ refer to TSSs, WESSs and trains power flow equations, respectively.

6. Online centralised control

The central controller adopts optimal control strategies framed as Optimal Traction Power Flow (OTPF), with objective functions and constraints tailored to the specific application. However, regardless of the objective function, these optimisation problems are characterised as large-scale, highly constrained, non-linear, and non-convex [42], primarily due to the inherent complexity of the power flow equations, which capture the physics of the problem.

In the following, two alternative online centralised control strategies are proposed. They assume controllable variables, such as the trains' regenerative power, WESS and reversible TSSs absorbed/injected power. Therefore, the dynamics of the trains are not affected by the optimisation procedure, which treats the train dynamics as a constraint of the problem. Furthermore, it is essential to highlight that the online implementation of these strategies entails the central controller acquiring real-time data from the field, solving an optimisation problem at each sample time k, and subsequently providing set points to local controllers. Consequently, in the following discussion, the superscript (k) denotes the generic sample of the time-varying variable involved in the optimisation procedure.

It is worth noting that the implementation of the centralised control paradigm requires a data exchange platform, which inherently experiences delays due to measurements and communication links. Notably, these time delays might compromise system stability and need to be carefully analysed to design a robust controller [43]. However, [29] concluded that, under normal operating conditions, communication delays meet the requirements for real-time control. Therefore, the control strategies proposed here, as is typical in the development of control strategies for smart grids, neglect this aspect since they are aimed at providing a suitable high-level control framework for the energy management of the railway system.

6.1. Strategy 1

This strategy focuses on a URS supplied by diode-based TSSs and equipped with WESSs. Consequently, the controllable variables consist of the train regenerative power injected into the network and the charging/discharging power of the WESSs. This entails determining, each sample time, the optimal set of values for the decision variables $\hat{\boldsymbol{\Gamma}}^{(k)}_{\mathrm{OTPF}}$:

$$\hat{\boldsymbol{\Gamma}}^{(k)}_{\mathrm{OTPF}} = \left\{\hat{\mathbf{V}}^{(k)}_{\mathcal{S}}, \hat{\mathbf{V}}^{(k)}_{\mathcal{B}}, \hat{\mathbf{V}}^{(k)}_{\mathcal{R}}, \hat{\mathbf{P}}^{(k)}_{\mathcal{S}}, \hat{\mathbf{P}}^{(k)}_{\mathcal{B}}, \hat{\mathbf{P}}^{(k)}_{\mathcal{R}}\right\} \tag{7}$$

aiming to minimise the energy dissipated through rheostatic braking. This leads to the following optimisation problem, where the objective is

$$\hat{\boldsymbol{\Gamma}}^{(k)}_{\mathrm{OTPF}} = \arg\min \mathbf{P}^{(k)T}_{\mathrm{rheo}}\mathbf{P}^{(k)}_{\mathrm{rheo}} \tag{8}$$

and the following constraints must be met:

$$\mathbf{F}^{(k)} = \mathbf{0} \tag{9}$$

$$\mathbf{V}^{(k)}_{\mathcal{S}} = \mathbf{V}_0 \tag{10}$$

$$\mathbf{P}^{(k)}_{\mathcal{R}_{\mathrm{tr}}} = \mathbf{P}^{\mathrm{ref},(k)}_{\mathcal{R}_{\mathrm{tr}}} \tag{11}$$

$$\mathbf{0} \le \mathbf{P}^{(k)}_{\mathcal{R}_{\mathrm{br}}} \le \mathbf{P}^{\mathrm{ref},(k)}_{\mathcal{R}_{\mathrm{br}}} \tag{12}$$

$$\mathbf{P}^{(k)}_{\mathcal{S}} \le \mathbf{P}^{\max}_{\mathcal{S}} \tag{13}$$

$$\mathbf{P}^{\mathrm{ch,av},(k)}_{\mathcal{B}} \le \mathbf{P}^{(k)}_{\mathcal{B}} \le \mathbf{P}^{\mathrm{dis,av},(k)}_{\mathcal{B}} \tag{14}$$

$$\mathbf{V}^{\min}_{\mathcal{R}} \le \mathbf{V}^{(k)}_{\mathcal{R}} \le \mathbf{V}^{\max}_{\mathcal{R}} \tag{15}$$

$$\mathbf{V}^{\min}_{\mathcal{B}} \le \mathbf{V}^{(k)}_{\mathcal{B}} \le \mathbf{V}^{\max}_{\mathcal{B}} \tag{16}$$

(9) is a non-linear equality constraint expressing the power flow equations, whereas (10) fixes the TSSs off-load voltage. Moreover, (11) accounts for the power delivered to trains, which must be supplied

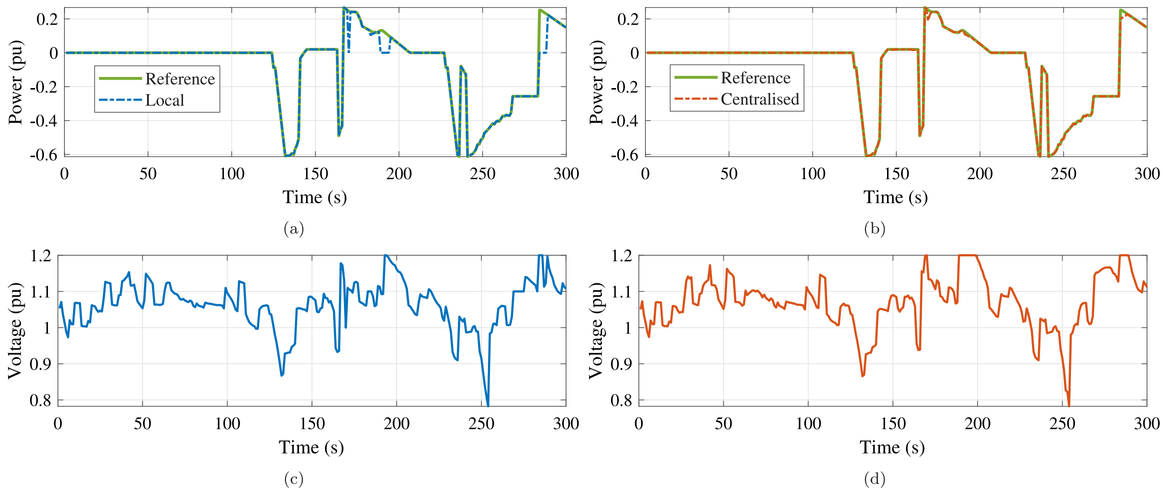

Fig. 10. Configuration A, Train #16: (a) and (c) refer to train power and voltage under local control, whereas (b) and (d) show the same quantities for the configuration under the centralised Strategy 1.

in order to avoid affecting their motion. On the contrary, braking energy becomes the subject of optimisation. Depending on the network's electrical state, the central controller determines, for each train, the allowable braking energy injection, as described in (12). Additionally, (13) and (14) impose limits on the power supplied by TSSs and the charging and discharging power of WESSs, respectively. Lastly, the voltage for both trains and WESSs must adhere to a specified range, as prescribed by (15) and (16). It is important to note that the WESS maximum charging and discharging power depend on its State of Charge (SoC). Specifically, they can be computed as follows:

$$P_b^{\mathrm{ch,av},(k)} = \max\left(\frac{E_b\left(SoC_b^{(k)} - SoC_{\max}\right)}{\eta_b^{\mathrm{ch}}\Delta T}, P_b^{\mathrm{ch,nom}}\right) \tag{17}$$

$$P_b^{\mathrm{dis,av},(k)} = \min\left(\eta_b^{\mathrm{dis}}\frac{E_b\left(SoC_b^{(k)} - SoC_{\min}\right)}{\Delta T}, P_b^{\mathrm{dis,nom}}\right) \tag{18}$$

where ΔT is the amplitude of the time-step discretisation employed for the optimisation. $SoC_{\max}$ and $SoC_{\min}$ indicate the maximum and minimum allowable value of SoC for the WESS, whereas E_b denotes the rated capacity of the bth WESS. Moreover, η_b^{ch} and η_b^{dis} stand for the efficiency during the charging and discharging phase, respectively, whereas $P_b^{\mathrm{ch,nom}}$ and $P_b^{\mathrm{dis,nom}}$ are the rated value for the charging and discharging power.

6.2. Strategy 2

This strategy is specifically tailored for systems powered by reversible TSSs. Noteworthy, the latter offers the possibility to regulate the output voltage and, consequently, the power exchanged with the AC grid. Thus, this strategy considers the TSSs' voltage and the power injected into the network by braking trains as optimisation variables. Notably, the possibility for dynamic adjustment of substation voltages results in improved system flexibility and resilience against sudden electric load variations. In other words, this strategy assumes the TSSs' voltage and the trains' regenerative braking energy as controllable variables. By solving the optimisation problem described below, the optimal setpoints for these variables are determined and dispatched to the local controllers, which are responsible for tracking the reference setpoints provided by the central controller. Hence, the optimisation problem is stated as:

$$\hat{\Gamma}_{\mathrm{OTPF}}^{(k)} = \arg\min \sum_{s\in\mathcal{S}} P_s^{(k)} \tag{19}$$

It is important to note that, in contrast with the strategies outlined above, $P_{\mathcal{S}}$ incorporates both positive and negative components due to the reversible nature of the substations. Therefore, the utilisation of an objective function such as (19) is geared towards minimising the positive components, which represent the power drawn from the AC grid while maximising the magnitude of negative components, which represent the power fed back into the AC grid.

The set of decision variables is defined as follows:

$$\hat{\Gamma}_{\mathrm{OTPF}}^{(k)} = \left\{\hat{\mathbf{V}}_{\mathcal{S}}^{(k)}, \hat{\mathbf{V}}_{\mathcal{B}}^{(k)}, \hat{\mathbf{V}}_{\mathcal{R}}^{(k)}, \hat{\mathbf{P}}_{\mathcal{S}}^{(k)}, \hat{\mathbf{P}}_{\mathcal{B}}^{(k)}, \hat{\mathbf{P}}_{\mathcal{R}}^{(k)}\right\} \tag{20}$$

The optimisation problem must meet the following constraints:

$$\mathbf{F}^{(k)} = \mathbf{0} \tag{21}$$

$$\mathbf{P}_{\mathcal{B}}^{(k)} = \mathbf{0} \tag{22}$$

$$\mathbf{P}_{\mathcal{R}_{\mathrm{tr}}}^{(k)} = \mathbf{P}_{\mathcal{R}_{\mathrm{tr}}}^{\mathrm{ref},(k)} \tag{23}$$

$$\mathbf{0} \le \mathbf{P}_{\mathcal{R}_{\mathrm{br}}}^{(k)} \le \mathbf{P}_{\mathcal{R}_{\mathrm{br}}}^{\mathrm{ref},(k)} \tag{24}$$

$$\mathbf{P}_{\mathcal{S}}^{\min} \le \mathbf{P}_{\mathcal{S}}^{(k)} \le \mathbf{P}_{\mathcal{S}}^{\max} \tag{25}$$

$$\mathbf{V}_{\mathcal{S}}^{\min} \le \mathbf{V}_{\mathcal{S}}^{(k)} \le \mathbf{V}_{\mathcal{S}}^{\max} \tag{26}$$

$$\mathbf{V}_{\mathcal{R}}^{\min} \le \mathbf{V}_{\mathcal{R}}^{(k)} \le \mathbf{V}_{\mathcal{R}}^{\max} \tag{27}$$

Compared to the previous strategy, the inclusion of reversible substations leads to changes in constraints (25) and (26). They are now introduced to limit reverse power flow based on the converter size, local energy sale policies and receptivity of the AC grid. Additionally, the off-load voltage of TSS is no longer fixed but has become a controllable variable, which must be maintained within prescribed limits. Noteworthy, the absence of WESSs results in imposing (22). Regarding constraints (21), (23) and (24) the same considerations made for Strategy 1 hold.

7. Numerical results

The effectiveness of the proposed centralised strategies is evaluated using the Naples Metro Line 1 as a real case study. This metro line connects the northwest area of the town with the southeast. It encompasses a total of 19 stations and spans an approximate distance of 36 km (18 km per direction), covered by trains in approximately 80 min. Currently, the railway service operates with a 10-min headway, significantly under-utilising the railway system originally designed for a theoretical 3-min headway. Therefore, to emphasise the effectiveness of the proposed approach, the present study assumes an increased railway service frequency of 5 min. According to the cyclical service model, this value of headway requires a fleet of 16 trains.

Table 1
Case A: Local vs. Centralised.

	Local	Centralised (Strategy 1)
WESSs (18 kWh/800 kW)	Grid-following (characteristic in Fig. 7): - Dead-band: $V_b \in [1.08, 1.12]$ pu - Constant charging power: $V_b > 1.12$ pu - Constant discharging power: $V_b < 1.08$ pu	By solving (8)
Train	Grid-following	By solving (8)
Diode-based TSS (7 MW)	Droop-controlled grid-forming - Equivalent resistance: $R_{\mathrm{TSS}} = 0.0190\ \Omega$ - Off-load voltage: $V_s = 1.1$ pu	By solving (8)

Table 2
Case B: Local vs. Centralised.

	Local	Centralised (Strategy 2)
Train	Grid-following	By solving (19)
Inverter-based TSS (7 MW)	Droop-controlled grid-forming - Virtual resistance: $R_{\mathrm{TSS}} = 0.0190\ \Omega$ - Off-load voltage: $V_s = 1.1$ pu	By solving (19)

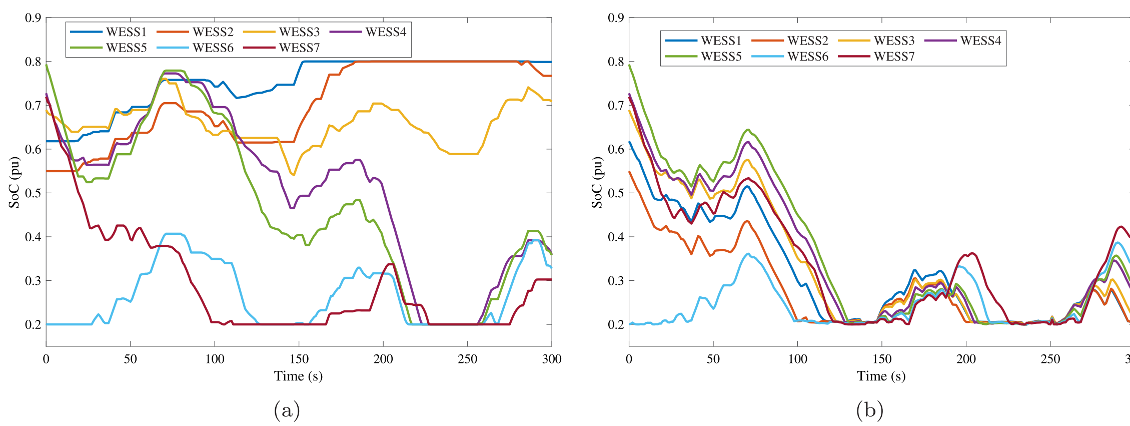

Fig. 11. Wayside SoC over time: (a) under local control, (b) under strategy 1.

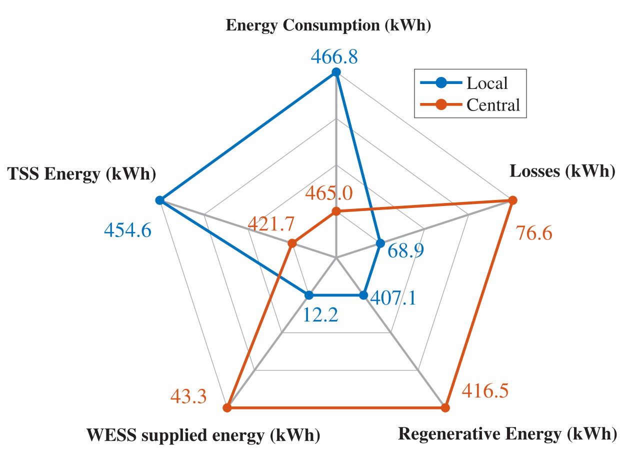

Fig. 12. Configuration A: comparison between the local control and Strategy 1. The amount of energy refers to 5 min.

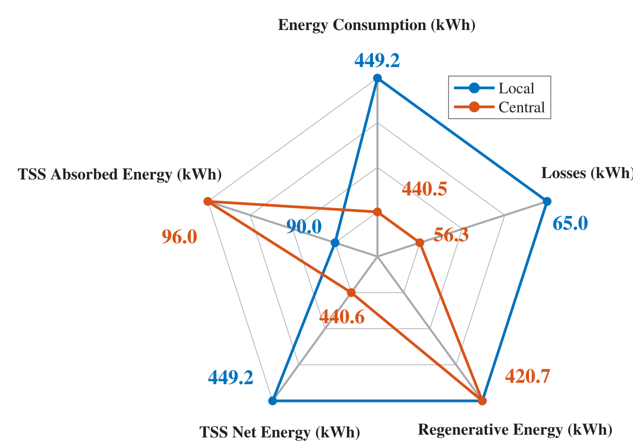

Fig. 13. Configuration B: comparison between the local control and Strategy 2. The amount of energy refers to 5 min.

The train reference profiles, which describe power and space over time, are determined using the software OpenTrack. These are the input variables of the optimisation problem. These profiles are influenced by various factors, including the train's performance characteristics, such as maximum speed (e.g., 80 km/h), maximum acceleration and deceleration (e.g., 1.1 m/s^2 and 1.1 m/s^2), as well as traction force limits and route characteristic.

The traction network operates at 1500 V, with a maximum allowable over-voltage of 1800 V (i.e., +20%), and a minimum allowable voltage of 1050 V (i.e., −30%). The MV distribution grid supplies the

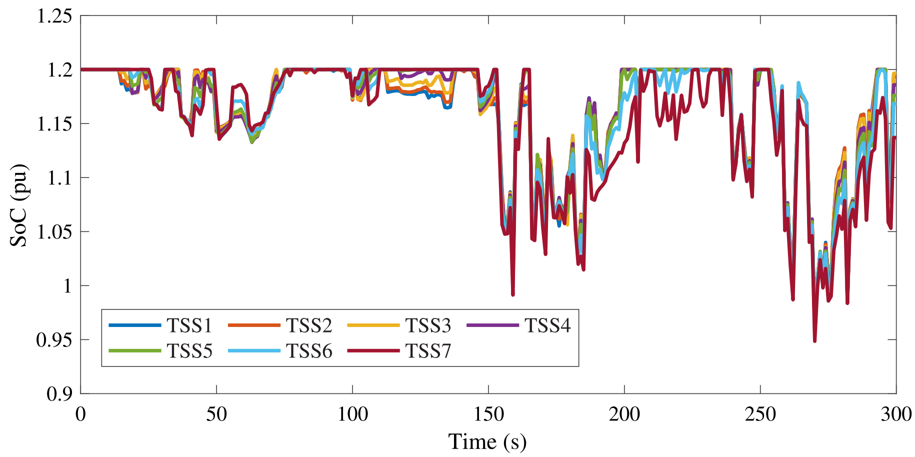

Fig. 14. Configuration B, Strategy 2: optimised TSSs off-load voltage over time.

system through seven diode-based TSSs (further details are provided in [41]). Moreover, the steady-state analysis of the railway network involves power flow calculations that are carried out in a per-unit system. The reference values for power and voltage are set at 7 MW and 1500 V, respectively.

The numerical analysis aims to show the advantages introduced by centralised control over conventional local control. To this end, two different system configurations have been considered:

- Configuration A: the URS is supplied through diode-based TSSs equipped with WESSs.
- Configuration B: the URS is supplied through inverter-based TSSs without any storage device.

In this regard, Tables 1 and 2 summarise the main information concerning the numerical comparison outlined in this section between conventional local control and the proposed centralised control strategies. Specifically, Configuration A has been analysed under the local control according to which WESS and trains behave as grid-following resources, whereas the TSSs act as grid-forming ones. Notably, the main parameters of the WESS static control characteristic are provided. Additionally, the results of this control paradigm have been compared with those provided by Strategy 1 applied to Configuration A. Similarly, the performance of the conventional local control and the proposed Strategy 2 have been compared when applied to Configuration B.

The simulations are carried out over a time horizon of 5 min which coincides with the assumed headway. A sample time of one second has been assumed. This means that, in the case of local control, the power flow problem is solved every second using the Matlab routine *fsolve*. Similarly, under Strategies 1 and 2, the set points of the local controllers are updated by solving the centralised optimisation problem every second using the Matlab routine *fmincon*.

7.1. Configuration A

This configuration features a WESS installed in parallel at each TSS. The initial SoC value of each WESS has been selected randomly according to a uniform distribution function over the interval $[0.2, 0.8]$ pu. Then, to ensure a fair comparison between the local control paradigm and Strategy 1, the same initial SoC values, so selected, have been used for both the simulation of local control and Strategy 1.

As an example, Fig. 10 shows a train's power profile (i.e., train #16) and the related catenary voltage under both local and centralised control. Specifically, the left side refers to the configuration under local control, whereas the right side shows results under Strategy 1. The solid green line in Fig. 10(a) denotes the reference power, which serves as input for the analysis. Specifically, the negative part accounts for the power required by the train for its motion, whereas the positive power represents the available regenerative power. Moreover, the blue dotted line represents the actual train power profile obtained by implementing the conventional local control. Due to the limited receptivity of the network, the train cannot utilise all the regenerative power theoretically available during the braking phase. Indeed, as shown in Fig. 10(c) the train voltage reaches repeatedly the maximum allowable voltage value. At these specific time instances, the train's over-voltage protection system activates, leading to the interruption of train regenerative power. Hence, the limited receptivity of the network makes the complete recovery of regenerative braking energy unattainable. Conversely, in the case of Strategy 1, as shown in Fig. 10(b) most of the regenerative energy is recovered. Furthermore, Fig. 11 illustrates the different behaviour of the WESSs under local control compared to Strategy 1. Notably, the coordinated actions provided by the central controller allow to significantly improve the receptivity of the network. Indeed, as detailed in the chart in Fig. 12, Strategy 1 yields approximately 2 kWh of energy savings over 5 min, primarily attributed to the increased network receptivity. The regenerative energy savings have increased from approximately 407 kWh to 416 kWh. However, it is worth noting that, compared with the centralised approach, the system under local control exhibits lower energy losses. This is due to the local control paradigm, which tends to bring the system closer to the over-voltage limits more frequently, resulting in lower currents.

7.2. Configuration B

Fig. 13 summarises the main results in terms of energy consumption. Notably, even when invertible TSSs, operate under local control, they enable the recovery of all regenerative braking energy. The surplus of energy, which is not used to power trains, can be fed back to the AC grid, provided that TSSs do not approach their power exchange limits. This is the case under study. On the other side, Strategy 2 is responsible for defining the optimal set-points for both TSSs' output voltage and the power that each train can inject into the network. These two control parameters are strategically utilised to enhance the network's receptivity and subsequently reduce its energy losses. Similar to the scenario with local control, Strategy 2 ensures complete regenerative braking recovery and a noteworthy reduction in energy consumption by nearly 9 kWh. Notably, the power exchanged with the AC grid increases by 6 kWh. The main difference lies in the management of TSSs' output voltage. Indeed, under local control, an increased TSS output voltage would lead to a significant reduction of the network receptivity, resulting in worse performance. Conversely, the centralised approach allows adjusting separately each substation's voltage, which is increased and lowered depending on the different operating conditions. To illustrate this, Fig. 14 shows how Strategy 2 regulates the TSSs off-load voltage

Table 3
Timing performance.

	Strategy 1	Strategy 2
μ	0.013 s	0.018 s
σ	0.015 s	0.013 s
Variables	53	30
Nonlinear inequality	7	8
Nonlinear equality	23	19
Linear equality	19	0
Upper bounds	53	30
Lower bounds	53	30
Termination tolerance	1E−4	1E−4

based on system operations. In contrast, the local control maintains this value at a constant level (e.g., 1.1 pu). Notably, the ability to control the TSSs' output voltage significantly increases system flexibility, leading to the improved performance shown earlier in Fig. 13.

8. Conclusion

The present study focused into the implementation of smart urban rail systems, focusing on the development of two distinct centralised control strategies tailored to specific system configurations. One strategy is tailored for a traction system supplied by diode-based TSS equipped with WESS, whereas the other targets a system supplied by inverter-based substations. These strategies optimise the management of the train's regenerative braking, WESS charging/discharging power, and TSS output voltage to minimise the system energy consumption. It is important to note that the application of the proposed approach requires a transition towards a more digitalised railway system, involving the massive exchange of data and information from the field to the ground. However, modern railway systems are already partially equipped with tools and devices used for signalling purposes. Therefore, applying a centralised control paradigm would not require a drastic change. Furthermore, numerical analyses on a real-case study demonstrated the effectiveness of the proposed strategies with significant energy savings.

Future works will thoroughly investigate the technological aspects related to the implementation of these strategies. The effects of time delays on system stability and the possible development of compensation measures will be analysed. Furthermore, other control paradigms featuring a lower computation burden, such as the distributed multi-agent solution, will be explored.

CRediT authorship contribution statement

Antonio Di Pasquale: Writing – original draft, Software, Methodology, Investigation, Formal analysis, Data curation, Conceptualization. **Mario Pagano:** Writing – review & editing, Writing – original draft, Supervision, Methodology, Conceptualization.

Declaration of competing interest

The authors declare that they have no known competing financial interests or personal relationships that could have appeared to influence the work reported in this paper.

Appendix

All simulations are run on the same laptop computer, namely a MacBook Air 2022 with an Apple M2 CPU, 8 GB RAM, a 10-core GPU, and a 512 GB SSD. As shown in Table 3, the execution time of both Strategy 1 and Strategy 2 is well below the sample time of one second. Indeed, they exhibit an average execution time μ of 0.013 s and 0.018 s, respectively, with a standard deviation σ of 0.015 s and 0.013 s. Specifically, these results refer to the time employed to solve the optimisation problem at kth time instant. The statistical analysis was conducted over 300 time instants with a termination tolerance of 1E−4 (note that the analysis is performed in per-unit, hence per-unit voltage and power values are known with an accuracy of 1E−4). Additional information, such as the number of variables and constraints, is available in Table 3.

Data availability

Data will be made available on request.

References

[1] Lerner W, Audenhove vF, et al. The future of urban mobility: Towards networked, multimodal cities in 2050. Public Transp Int 2012;(2).
[2] Navarro L, Fernandez-Cardador A, Cucala A. Design of indicators to guide capacity improvements in urban railway lines. J Urban Mobil 2021;1:100003.
[3] Pietrzak K, Pietrzak O, Montwiłł A. Light freight railway (LFR) as an innovative solution for sustainable urban freight transport. Sustain Cities Soc 2021;66:102663.
[4] Barrero R, Van Mierlo J, Tackoen X. Energy savings in public transport. IEEE Veh Technol Mag 2008;3(3):26–36.
[5] Barrero R, Tackoen X, Van Mierlo J. Stationary or onboard energy storage systems for energy consumption reduction in a metro network. Proc Inst Mech Eng Part F: J Rail Rapid Transit 2010;224(3):207–25.
[6] Domínguez M, Cucala A, Fernández A, Pecharromán R, Blanquer J. Energy efficiency on train control: design of metro ATO driving and impact of energy accumulation devices. In: 9th world congress on railway research–WCRR. vol. 2011, 2011.
[7] Chymera M, Renfrew A, Barnes M. Analyzing the potential of energy storage on electrified transit systems. In: 8th world congress of railway research–WCRR. vol. 2008, 2008.
[8] Destraz B, Barrade P, Rufer A, Klohr M. Study and simulation of the energy balance of an urban transportation network. In: 2007 European conference on power electronics and applications. IEEE; 2007, p. 1–10.
[9] Moskowitz J-P, Cohuau J-L. STEEM: ALSTOM and RATP experience of supercapacitors in tramway operation. In: 2010 IEEE vehicle power and propulsion conference. IEEE; 2010, p. 1–5.
[10] Meishner F, Sauer DU. Wayside energy recovery systems in DC urban railway grids. eTransportation 2019;1:100001.
[11] Teymourfar R, Asaei B, Iman-Eini H, et al. Stationary super-capacitor energy storage system to save regenerative braking energy in a metro line. Energy Convers Manage 2012;56:206–14.
[12] Lee H, Song J, Lee H, Lee C, Jang G, Kim G. Capacity optimization of the supercapacitor energy storages on DC railway system using a railway powerflow algorithm. Int J Innov Comput Inf Control 2011;7(5):2739–53.
[13] Cornic D. Efficient recovery of braking energy through a reversible dc substation. In: Electrical systems for aircraft, railway and ship propulsion. IEEE; 2010, p. 1–9.
[14] Zhang G, Tian Z, Tricoli P, Hillmansen S, Wang Y, Liu Z. Inverter operating characteristics optimization for DC traction power supply systems. IEEE Trans Veh Technol 2019;68(4):3400–10.
[15] Zhang G, Qian J, Zhang X. Application of a high-power reversible converter in a hybrid traction power supply system. Appl Sci 2017;7(3):282.
[16] Chavali P, Yang P, Nehorai A. A distributed algorithm of appliance scheduling for home energy management system. IEEE Trans Smart Grid 2014;5(1):282–90.
[17] Zhao Z, Lee WC, Shin Y, Song K-B. An optimal power scheduling method for demand response in home energy management system. IEEE Trans Smart Grid 2013;4(3):1391–400.
[18] Costanzo GT, Zhu G, Anjos MF, Savard G. A system architecture for autonomous demand side load management in smart buildings. IEEE Trans Smart Grid 2012;3(4):2157–65.
[19] Khayyam S, Ponci F, Goikoetxea J, Recagno V, Bagliano V, Monti A. Railway energy management system: Centralized–decentralized automation architecture. IEEE Trans Smart Grid 2015;7(2):1164–75.
[20] Zhang R. Research on an intelligent management and supervision system for a high-speed railway interlocking test. IEEE Access 2024.
[21] Araúz J, Martinez S. Methodology for assessing the impact of regenerative braking energy injection of a direct current railway system on the distribution grid. Electr Power Syst Res 2023;220:109368.
[22] Nash C. Passenger railway reform in the last 20 years–European experience reconsidered. Res Transp Econ 2008;22(1):61–70.
[23] Cantos-Sanchez P, Moner-Colonques R, Sempere-Monerris JJ. Market power of railway operators under different vertical structures. Transp Econ Manag 2023.
[24] de la Fuente EP, Mazumder SK, Franco IG. Railway electrical smart grids: An introduction to next-generation railway power systems and their operation. IEEE Electrif Mag 2014;2(3):49–55.

[25] EU 7th Framework programme. Merlin. 2023, https://web.archive.org/web/20170530213945/http://www.merlin-rail.eu/?page_id=56. [Accessed 27 October 2023].
[26] Şengör İ, Kılıçkıran HC, Akdemir H, Kekezoğlu B, Erdinc O, Catalao JP. Energy management of a smart railway station considering regenerative braking and stochastic behaviour of ESS and PV generation. IEEE Trans Sustain Energy 2017;9(3):1041–50.
[27] Rigaut T, Carpentier P, Chancelier JP, De Lara M, Waeytens J. Stochastic optimization of braking energy storage and ventilation in a subway station. IEEE Trans Power Syst 2018;34(2):1256–63.
[28] Chen J, Zhao Y, Wang M, Wang K, Huang Y, Xu Z. Power sharing and storage-based regenerative braking energy utilization for sectioning post in electrified railways. IEEE Trans Transp Electrif 2023.
[29] Chen J, Ge Y, Wang K, Hu H, He Z, Tian Z, Li Y. Integrated regenerative braking energy utilization system for multi-substations in electrified railways. IEEE Trans Ind Electron 2022;70(1):298–310.
[30] Dong H, Tian Z, Spencer JW, Fletcher D, Hajiabady S. Coordinated control strategy of railway multisource traction system with energy storage and renewable energy. IEEE Trans Intell Transp Syst 2023;24(12):15702–13.
[31] Khayyam S, Berr N, Razik L, Fleck M, Ponci F, Monti A. Railway system energy management optimization demonstrated at offline and online case studies. IEEE Trans Intell Transp Syst 2018;19(11):3570–83.
[32] Razik L, Berr N, Khayyam S, Ponci F, Monti A. REM-S–railway energy management in real rail operation. IEEE Trans Veh Technol 2018;68(2):1266–77.
[33] Kleftakis VA, Hatziargyriou ND. Optimal control of reversible substations and wayside storage devices for voltage stabilization and energy savings in metro railway networks. IEEE Trans Transp Electrif 2019;5(2):515–23.
[34] Unamuno E, Barrena JA. Hybrid ac/dc microgrids—Part II: Review and classification of control strategies. Renew Sustain Energy Rev 2015;52:1123–34.
[35] Zuo Y, Yuan Z, Sossan F, Zecchino A, Cherkaoui R, Paolone M. Performance assessment of grid-forming and grid-following converter-interfaced battery energy storage systems on frequency regulation in low-inertia power grids. Sustain Energy Grids Netw 2021;27:100496.
[36] Serrano-Jiménez D, Castano-Solís S, Unamuno E, Barrena J. Droop control operation strategy for advanced DC converter-based electrical railway power supply systems for high-speed lines. Int J Electr Power Energy Syst 2022;137:107870.
[37] Arboleya P, Mohamed B, González-Morán C, El-Sayed I. BFS algorithm for voltage-constrained meshed DC traction networks with nonsmooth voltage-dependent loads and generators. IEEE Trans Power Syst 2015;31(2):1526–36.
[38] Mayet C, Horrein L, Bouscayrol A, Delarue P, Verhille J-N, Chattot E, Lemaire-Semail B. Comparison of different models and simulation approaches for the energetic study of a subway. IEEE Trans Veh Technol 2013;63(2):556–65.
[39] Arboleya P, Coto M, González-Morán C, Arregui R. On board accumulator model for power flow studies in DC traction networks. Electr Power Syst Res 2014;116:266–75.
[40] Yu J, Goodman C. Modelling of rail potential rise and leakage current in DC rail transit systems. In: IEE colloquium on stray current effects of DC railways and tramways. IET; 1990, 2–2.
[41] Botte M, D'Acierno L, Di Pasquale A, Mottola F, Pagano M. Optimal motion of a rolling stock fleet under traction power system constraints. IEEE Trans Transp Electrif 2022;9(1):1554–63.
[42] Ghasemi M, Ghavidel S, Akbari E, Vahed AA. Solving non-linear, non-smooth and non-convex optimal power flow problems using chaotic invasive weed optimization algorithms based on chaos. Energy 2014;73:340–53.
[43] Mehdi M, Kim C-H, Saad M. Robust centralized control for DC islanded microgrid considering communication network delay. IEEE Access 2020;8:77765–78.